

# Polarized Single Top Quark Production in $e\gamma$ Collision and Anomalous $Wtb$ Couplings

B. Şahin\* and İ. Şahin†

*Department of Physics, Faculty of Sciences,  
Ankara University, 06100 Tandogan, Ankara, Turkey*

## Abstract

We investigate the potential of  $e\gamma$  collisions to probe anomalous  $Wtb$  couplings via the polarized single top quark production process  $e^+\gamma \rightarrow t\bar{b}\bar{\nu}_e$ . We find 95% confidence level limits on the anomalous coupling parameters  $F_{2L}$  and  $F_{2R}$  with an integrated luminosity of  $500fb^{-1}$  and  $\sqrt{s} = 0.5, 1$  and  $1.5$  TeV energies. The effects of top quark spin polarization on the anomalous  $Wtb$  couplings are discussed. It is shown that polarization leads to a considerable improvement in the sensitivity limits.

PACS numbers: 14.65.Ha, 13.88.+e

arXiv:0709.0365v2 [hep-ph] 24 Feb 2008

---

\*dilec@science.ankara.edu.tr

†isahin@science.ankara.edu.tr

## I. INTRODUCTION

The standard model (SM) has been tested with good accuracy and it has been proved to be successful in the energy scale of the present colliders. However, it is generally believed that SM is embedded in a more fundamental theory (new physics) in which its effects can be observed at higher energy scales. The top quark is the heaviest fermion in the SM. Its mass is at the electroweak symmetry-breaking scale. Because of its large mass, the top quark and its couplings are expected to be more sensitive to new physics than other particles [1]. Therefore precision measurements of top quark couplings will be the crucial test of the structure of the SM. A deviation of the couplings from the expected values would indicate the existence of new physics beyond the SM.

In this work we analyzed anomalous  $Wtb$  and  $\gamma Wtb$  couplings in the single top production process  $e^+\gamma \rightarrow t\bar{b}\bar{\nu}_e$ . Since the top quark is very heavy, its weak decay time is much shorter than the typical time for the strong interactions to affect its spin [2]. Therefore the information on its polarization is not disturbed by hadronization effects but transferred to the decay products. The angular distribution of the top quark decay involves correlations between top decay products and top quark spin:

$$\frac{1}{\Gamma_T} \frac{d\Gamma}{d\cos\theta} = \frac{1}{2}(1 + A_{\uparrow\downarrow}\alpha\cos\theta) \quad (1)$$

Here the dominant decay chain of the top quark in the standard model  $t \rightarrow W^+b(W^+ \rightarrow l^+\nu, \bar{d}u)$  is considered.  $A_{\uparrow\downarrow}$  is the spin asymmetry and  $\theta$  is defined as the angle between top quark decay products and the top quark spin quantization axis in the rest frame of the top quark.  $\alpha$  is the correlation coefficient and  $\alpha = 1$  for  $l$  or  $\bar{d}$ , which leads to the strongest correlation. We take into account top quark spin polarization along the direction of various spin bases to improve the sensitivity limits.

Anomalous  $Wtb$  and  $\gamma Wtb$  couplings can be analyzed in a model independent way by means of the effective Lagrangian approach [3, 4, 5, 6]. We consider the following couplings, which are necessary for the process  $e^+\gamma \rightarrow t\bar{b}\bar{\nu}_e$ .

$$L = \frac{g_w}{\sqrt{2}}[W_\mu\bar{t}(\gamma^\mu F_{1L}P_- + \gamma^\mu F_{1R}P_+)b - \frac{1}{2m_w}W_{\mu\nu}\bar{t}\sigma^{\mu\nu}(F_{2L}P_- + F_{2R}P_+)b] + h.c. \quad (2)$$

where

$$\begin{aligned}
W_{\mu\nu} &= D_\mu W_\nu - D_\nu W_\mu \quad , \quad D_\mu = \partial_\mu - ieA_\mu \\
P_{\mp} &= \frac{1}{2}(1 \mp \gamma_5) \quad , \quad \sigma^{\mu\nu} = \frac{i}{2}(\gamma^\mu\gamma^\nu - \gamma^\nu\gamma^\mu)
\end{aligned}
\tag{3}$$

In the SM, the (V-A) coupling  $F_{1L}$  corresponds to the Cabibbo-Kobayashi-Maskawa (CKM) matrix element  $V_{tb}$ , which is very close to unity and  $F_{1R}$ ,  $F_{2L}$  and  $F_{2R}$  are equal to zero. The (V+A) coupling  $F_{1R}$  is severely bounded by the CLEO  $b \rightarrow s\gamma$  data [7] at a level such that it will be out of reach at expected future colliders. Therefore we set  $F_{1L} = 0.999$  and  $F_{1R} = 0$  as required by present data [8]. The magnetic type anomalous couplings are related to the coefficients  $C_{tW\Phi}$  and  $C_{bW\Phi}$  [5] in the general effective lagrangian by

$$F_{2L} = \frac{C_{tW\Phi}\sqrt{2}vm_w}{\Lambda^2g} \quad F_{2R} = \frac{C_{bW\Phi}\sqrt{2}vm_w}{\Lambda^2g}
\tag{4}$$

where  $\Lambda$  is the scale of new physics. Natural values of the couplings  $F_{2L(R)}$  are in the region [1] of

$$\frac{\sqrt{m_b m_t}}{v} \sim 0.1
\tag{5}$$

and do not exceed unitarity violation bounds for  $|F_{2L(R)}| \sim 0.6$  [4].

There are many detailed discussions in the literature for  $Wtb$  couplings in the single and pair top quark production. The single top quark production cross section for the process  $e^+e^- \rightarrow Wtb$  has been discussed below and the above the  $t\bar{t}$  threshold [9] and for the process  $e^+e^- \rightarrow e\bar{\nu}tb$  at CERN LEP2 [10] and linear  $e^+e^-$  collider [11] energies. Pair top production processes for a future linear collider have been investigated in  $e^+e^-$  and  $\gamma\gamma$  collisions [12].  $Wtb$  couplings have also been investigated at Fermilab Tevatron and CERN LHC [13, 14]. In  $ep$  collision, the  $Wtb$  couplings were analyzed for polarized top quarks via the process  $ep \rightarrow t\bar{b}\bar{\nu} + X$  [15]. It was shown that polarization leads to a significant improvement in the sensitivity limits. In the literature there have been several studies of anomalous  $Wtb$  couplings in  $e\gamma$  collisions [16]. Different from these studies we take into account top quark spin polarization along the direction of various spin bases to improve the sensitivity limits.

## II. CROSS SECTIONS OF POLARIZED TOP QUARKS IN THE $e\gamma$ COLLISION

Research and development of linear  $e^+e^-$  colliders have been progressing and the physics potential of these future machines is under study. After linear colliders have been constructed their operating modes of  $e\gamma$  and  $\gamma\gamma$  are expected to be designed [17, 18]. A real gamma beam is obtained through Compton backscattering of laser light off a linear electron beam, where most of the photons are produced at the high energy region. The luminosities for  $e\gamma$  and  $\gamma\gamma$  collisions turn out to be of the same order as the one for  $e^+e^-$  [19], so the cross sections for photoproduction processes with real photons are considerably larger than the virtual photon case. In our calculations we consider three different center of mass energies  $\sqrt{s}=0.5, 1$  and  $1.5$  TeV of the parental linear  $e^+e^-$  collider.

The spectrum of the backscattered photons is given by [19]. We have

$$f_{\gamma/e}(y) = \frac{1}{g(\zeta)} \left[ 1 - y + \frac{1}{1-y} - \frac{4y}{\zeta(1-y)} + \frac{4y^2}{\zeta^2(1-y)^2} \right] \quad (6)$$

where

$$g(\zeta) = \left( 1 - \frac{4}{\zeta} - \frac{8}{\zeta^2} \right) \ln(\zeta + 1) + \frac{1}{2} + \frac{8}{\zeta} - \frac{1}{2(\zeta + 1)^2} \quad (7)$$

with  $\zeta = 4E_e E_0 / M_e^2$ .  $E_0$  is the energy of the initial laser photon and  $E_e$  is the energy of the initial electron beam before Compton backscattering.  $y$  is the fraction that represents the ratio of the scattered photon and initial electron energy for the backscattered photons moving along the initial electron direction. The maximum value of  $y$  reaches 0.83 when  $\zeta = 4.8$ , in which case the backscattered photon energy is maximized without spoiling the luminosity. The integrated cross section over the backscattered photon spectrum is given by

$$\sigma(s) = \int_{y_{min}}^{0.83} f_{\gamma/e}(y) \hat{\sigma}(\hat{s}) dy \quad (8)$$

where  $y_{min} = \frac{m_t^2}{s}$  and  $\hat{s}$  is the square of the center of mass energy of the subprocess  $e^+\gamma \rightarrow t\bar{b}\bar{\nu}_e$ .  $\hat{s}$  is related to  $s$ , the square of the center of mass energy of  $e^+e^-$ , by  $\hat{s} = ys$ .

In the SM single production of the top quark via the process  $e^+\gamma \rightarrow t\bar{b}\bar{\nu}_e$  is described by four tree level diagrams. Each of the diagrams contains a  $Wtb$  vertex and, due to its

V-A structure, the top quarks produced are highly polarized. It was shown in ref.[20] that the top quark possesses a high degree of spin polarization when its spin decomposition axis is along the incoming  $e^+$  beam. In the effective Lagrangian approach, there are five tree level diagrams; one of them contains an anomalous  $\gamma Wtb$  vertex, which is absent in the SM (Fig.1).

The top quark possesses a large mass, so its helicity is frame dependent and changes under a boost from one frame to another. The helicity and chirality states do not coincide with each other and there is no reason to believe that the helicity basis will give the best description of the spin of top quarks. Therefore it is reasonable to study other spin bases better than helicity for the top quark spin.

The spin four-vector of a top quark is defined by

$$s_t^\mu = \left( \frac{\vec{p}_t \cdot \vec{s}'}{m_t}, \vec{s}' + \frac{\vec{p}_t \cdot \vec{s}'}{m_t(E_t + m_t)} \vec{p}_t \right) \quad (9)$$

where  $(s_t^\mu)_{RF} = (0, \vec{s}')$  in the top quark rest frame. Top quark spinors are the eigenstates of the operator  $\gamma_5(\gamma_\mu s_t^\mu)$ :

$$[\gamma_5(\gamma_\mu s_t^\mu)] u(p_t, \pm s) = \pm u(p_t, \pm s) \quad (10)$$

Using eq.(10) one can easily obtain the spin projection operator:

$$\hat{\Sigma}(s) = \frac{1}{2}(1 + \gamma_5(\gamma_\mu s_t^\mu)) \quad (11)$$

Therefore during amplitude calculations one should project the top quark spin onto a given spin direction. We consider four different top spin directions in the laboratory frame: the incoming positron beam, the photon beam directions and the outgoing  $\bar{b}$  direction and also the helicity basis.

The definition of the spin axis in the rest frame of the top quark does not depend on the coordinate frame in which the cross section is taken. So it is more convenient to calculate the cross section in the  $e^+e^-$  center of mass system (laboratory frame). In the top quark rest frame, its spin direction along any beam (positron, photon or  $\bar{b}$  beam) can be defined as follows:

$$\vec{s}^j = \lambda \frac{\vec{p}^*}{|\vec{p}^*|}, \quad \lambda = \pm 1. \quad (12)$$

Here,  $\vec{p}^*$  is the particle momentum (positron, photon or  $\bar{b}$ ), observed in the rest frame of the top quark. Since the particle momentum  $\vec{p}$  is first defined in the  $e^+e^-$  center of mass system in which the cross section is calculated,  $\vec{p}^*$  should be obtained by a Lorentz boost from the  $e^+e^-$  cm system:

$$\vec{p}^* = \vec{p} + \frac{\gamma - 1}{\beta^2}(\vec{\beta} \cdot \vec{p})\vec{\beta} - E\gamma\vec{\beta} \quad (13)$$

where  $\vec{\beta}$  is the velocity of the top quark in the  $e^+e^-$  cm system. In the cross section calculations we have performed a boost to obtain  $\vec{p}^*$  at each point in phase space.

One can see from Fig.2-5 the influence of the top quark spin polarizations on the deviations of the total cross sections from their SM value at  $\sqrt{s} = 1.5$  TeV. In these figures an up arrow  $\uparrow$  (down arrow  $\downarrow$ ) stands for spin up  $\lambda = +1$  (spin down  $\lambda = -1$ ), and "L" and "R" represent left and right helicity. These figures show that cross sections have a symmetric behavior as a function of the anomalous parameter  $F_{2R}$ . We see from Fig.4 that a polarized cross section is almost insensitive to the anomalous parameter  $F_{2R}$  at the  $\gamma$ -beam  $\downarrow$  spin polarization configuration. On the other hand the cross section at this polarization configuration is very sensitive to the anomalous parameter  $F_{2L}$ . Therefore the  $\gamma$ -beam  $\downarrow$  spin polarization configuration can be used to isolate the anomalous coupling parameter  $F_{2L}$ .

In our calculations phase space integrations have been performed by GRACE [21], which uses a Monte Carlo routine.

### III. ANGULAR CORRELATIONS BETWEEN TOP DECAY PRODUCTS AND TOP QUARK SPIN

Angular distributions of the top quark decay products have correlations with its spin polarizations. Let us consider the differential cross section for the complete process including subsequent top decay,

$$\begin{aligned}
d\sigma (e^+\gamma \rightarrow t\bar{b}\bar{\nu}_e \rightarrow b\ell^+\nu_\ell\bar{b}\bar{\nu}_e) = & \frac{1}{2s}|M|^2 \frac{d^3p_3}{(2\pi)^3 2E_3} \frac{d^3p_4}{(2\pi)^3 2E_4} \frac{d^3p_5}{(2\pi)^3 2E_5} \frac{d^3p_6}{(2\pi)^3 2E_6} \frac{d^3p_7}{(2\pi)^3 2E_7} \\
& \times (2\pi)^4 \delta^4 \left( \sum_i p_i - \sum_f p_f \right)
\end{aligned} \tag{14}$$

where  $p_i = p_1, p_2$  are the momenta of the incoming fermions and  $p_f = p_3, p_4, p_5, p_6, p_7$  are the momenta of the outgoing fermions.  $|M|^2$  is the square of the full amplitude, which is averaged over the initial spins and summed over the final spins. The full amplitude can be expressed as follows:

$$\begin{aligned}
|M|^2 (2\pi)^4 \delta^4 \left( \sum_i p_i - \sum_f p_f \right) = & \int \frac{d^4q}{(2\pi)^4} \left| \sum_{s_t} M_a(s_t) D_t(q^2) M_b(s_t) \right|^2 \\
& \times (2\pi)^4 \delta^4 (p_1 + p_2 - p_3 - p_4 - q) \\
& \times (2\pi)^4 \delta^4 (q - p_5 - p_6 - p_7)
\end{aligned} \tag{15}$$

Here  $q$  and  $s_t$  are the internal momentum and spin of the top quark.  $D_t(q^2)$  is the Breit-Wigner propagator factor. It is given by

$$D_t(q^2) = \frac{1}{q^2 - m_t^2 + im_t\Gamma_t} \tag{16}$$

$M_a(s_t)$  is the amplitude for the process  $e^+\gamma \rightarrow t\bar{b}\bar{\nu}_e$  with an on shell  $t$  quark.  $M_b(s_t)$  is the decay amplitude for  $t \rightarrow b\ell^+\nu_\ell$ . The square of the decay amplitude summed over the final fermion spins is given by

$$|M_b(s_t)|^2 = \frac{2g_w^4}{[(p_t - p_b)^2 - m_w^2]^2} (p_b \cdot p_t - p_b \cdot p_\ell)(p_\ell \cdot p_t - m_t(s_t \cdot p_\ell)) \tag{17}$$

By means of this amplitude one can easily obtain equation (1), the angular distribution of top quark decay.

Therefore, the full cross section has been written as a product of production and decay parts. One can show that interference terms from different spin states will vanish after integrating the decay part over azimuthal angles of top quark decay products. Then the following result can be reached:

$$d\sigma (e^+\gamma \rightarrow t\bar{b}\bar{\nu}_e \rightarrow b\ell^+\nu_\ell\bar{b}\bar{\nu}_e) = \left[ d\sigma (e^+\gamma \rightarrow \uparrow t\bar{b}\bar{\nu}_e) \frac{d\Gamma (\uparrow t \rightarrow b\ell^+\nu_\ell)}{\Gamma (t \rightarrow b\ell^+\nu_\ell)} + d\sigma (e^+\gamma \rightarrow \downarrow t\bar{b}\bar{\nu}_e) \frac{d\Gamma (\downarrow t \rightarrow b\ell^+\nu_\ell)}{\Gamma (t \rightarrow b\ell^+\nu_\ell)} \right] BR (t \rightarrow b\ell^+\nu_\ell) \quad (18)$$

where  $BR (t \rightarrow b\ell^+\nu_\ell)$  is the leptonic branching ratio for the top quark. Up and down arrows indicate the spin up and spin down cases along a specified spin quantization axis, respectively.  $d\Gamma (\uparrow t \rightarrow b\ell^+\nu_\ell)$  and  $d\Gamma (\downarrow t \rightarrow b\ell^+\nu_\ell)$  are differential decay rates for polarized top quarks. The unpolarized rate is given by;  $d\Gamma (t \rightarrow b\ell^+\nu_\ell) = d\Gamma (\uparrow t \rightarrow b\ell^+\nu_\ell) + d\Gamma (\downarrow t \rightarrow b\ell^+\nu_\ell)$ .

Top quark polarization can be determined by measuring the angular distribution of outgoing charged lepton in the top rest frame. It is possible to obtain from the expression (18) the polarized production cross section as a coefficient of the angular distribution by a fitting procedure. In this paper we ignore the problems associated with the reconstruction of the top rest frame. We assume that the top quark rest frame can be reconstructed.

#### IV. SENSITIVITY TO ANOMALOUS COUPLINGS

We have obtained 95% C.L. limits on the anomalous coupling parameters  $F_{2L}$  and  $F_{2R}$  using a  $\chi^2$  analysis at  $\sqrt{s} = 0.5, 1$  and  $1.5$  TeV and an integrated luminosity  $L_{int} = 500 fb^{-1}$  without systematic errors. The expected number of events has been calculated considering the leptonic channel of the W boson as the signal  $N = AL_{int}\sigma B(W \rightarrow l\nu)$ , where  $A$  is the overall acceptance. The limits for the anomalous coupling parameters are given in Table I-III for top quark spin polarization along the direction of various spin bases with the acceptance  $A = 0.85$ . One can see from these tables that the sensitivity to the anomalous parameter  $F_{2R}$  at the  $\gamma$ -beam  $\downarrow$  spin polarization configuration is the worst. This feature is reflected in Fig.4 too. On the other hand, the limits on  $F_{2R}$  are most sensitive at the  $\gamma$ -beam  $\uparrow$  spin polarization configuration. The  $\gamma$ -beam  $\uparrow$  improves the sensitivity limits by a factor of 1.4 at  $\sqrt{s} = 0.5$  TeV and by a factor of 1.5 at  $\sqrt{s} = 1$  TeV when compared to the unpolarized (total) case.

Lower and upper bounds on the anomalous parameter  $F_{2L}$  are not symmetric, as can be seen from the tables. Polarization leads to a significant improvement to these sensitivity bounds; the  $\bar{b}$ -beam  $\uparrow$  polarization configuration improves the lower bounds on  $F_{2L}$  by a factor of 2.7 at  $\sqrt{s} = 0.5$  TeV and by a factor of 2 at  $\sqrt{s} = 1$  TeV when compared with the



unpolarized (total) case. At  $\sqrt{s} = 0.5$  TeV,  $\bar{b}$ -beam  $\downarrow$  and helicity right improves the upper bound on  $F_{2L}$  by a factor of 1.75. These polarization configurations as well as  $\gamma$ -beam  $\uparrow$  leads to an improvement on the upper bound by a factor of 3.5 at  $\sqrt{s} = 1$  TeV. The most sensitive bounds are obtained at  $\sqrt{s} = 1.5$  TeV.  $\gamma$ -beam  $\uparrow$  and helicity right polarizations improve the upper bounds on  $F_{2L}$  by a factor of 5 when compared with the unpolarized case.

As a conclusion, we have obtained a considerable improvement in the sensitivity bounds by taking into account top quark spin polarization. Improved results by spin polarization in  $e\gamma$  colliders with a luminosity of  $500 \text{ fb}^{-1}$  have a higher potential to probe the  $F_{2L}$  and  $F_{2R}$  couplings than Tevatron and CERN LHC [14] and also than the  $ep$  collider TESLA+HERAp option [15]. Furthermore, the linear  $e^+e^-$  collider and its  $e\gamma$  mode provide a clean environment and the experimental clearness is an additional advantage of  $e\gamma$  collisions with respect to  $pp$ ,  $p\bar{p}$  and  $ep$  collisions.

- 
- [1] R. D. Peccei, X. Zhang, Nucl. Phys. **B337**, 269 (1990);  
R. D. Peccei, S. Peris and X. Zhang, Nucl. Phys. **B349**, 305 (1991).
- [2] I. Bigi, Y. Dokshitzer, V. Khoze, J. Kuhn and P. Zerwas, Phys. Lett. **B 181**, 157 (1986).
- [3] W. Buchmuller and D. Wyler, Nucl. Phys. **B268**, 621 (1986);  
K. Hagiwara, S. Ishihara, R. Szalapski and D. Zeppenfeld, Phys. Rev. **D48**, 2182 (1993).
- [4] G.J. Gounaris, F.M. Renard and C. Verzegnassi, Phys. Rev. **D52**, 451 (1995);  
G.J. Gounaris, F.M. Renard, and N.D. Vlachos, Nucl. Phys. **B459**, 51 (1996).
- [5] K. Whisnant, J. Yang, B. Young and X. Zhang, Phys. Rev. **D56**, 467 (1997);  
J. M. Yang and B. Young, Phys. Rev. **D56**, 5907 (1997).
- [6] G. Kane, G. Ladinsky and C.-P. Yuan, Phys. Rev. **D45**, 124 (1992).
- [7] M.S. Alam *et al.* (CLEO Collaboration), Phys. Rev. Lett. **74**, 2885 (1995);  
F. Larios, M.A. Perez and C.-P. Yuan Phys. Lett **B457**, 334 (1999).
- [8] D.E. Groom, *et al.*, Eur. Phys. J. **C 15**, 1 (2000).
- [9] S. Ambrosanio and B. Mele, Z. Phys. **C 63**, 63 (1994);  
N. V. Dokholian and G. V. Jikia, Phys. Lett. **B 336**, 251 (1994).
- [10] K. Hagiwara, M. Tanaka and T. Stelzer, Phys. Lett. **B 325**, 521 (1994);  
E. Boos *et al.*, Phys. Lett. **B 326**, 190 (1994).
- [11] E. Boos *et al.*, Z. Phys. **C 70**, 255 (1996);  
A. Bienarchik, K. Cieckiewicz and K. Kolodziej, hep-ph/012253.
- [12] B. Grzadkowski and Z. Hioki, Phys. Rev. **D 61**, 014013 (1999);  
B. Grzadkowski and Z. Hioki, Nucl. Phys. **B 585**, 3 (2000);  
B. Grzadkowski, Z. Hioki, K. Ohkuma and J. Wudka Phys. Lett. **B 593**, 189 (2004);  
P. Batra and T. M. P. Tait, Phys. Rev. **D 74**, 054021 (2006).
- [13] D. Dicus and S. Willenbrock, Phys. Rev. **D 34**, 155 (1986);  
C.-P. Yuan, Phys. Rev. **D 41**, 42 (1990);  
S. Cortese and R. Petronzio, Phys. Lett. **B 253**, 494 (1991);  
G. V. Jikia and S. R. Slabospitsky, Phys. Lett. **B 295**, 136 (1992);  
R. K. Ellis and S. Parke, Phys. Rev. **D 46**, 3785 (1992);  
G. Bordes and B. van Eijk, Z. Phys. **C 57**, 81 (1993);

- D. O. Carlson and C.-P. Yuan, Phys. Lett. **B 306**, 386 (1993);
- D. O. Carlson, E. Malkawi and C.-P. Yuan, Phys. Lett. **B 337**, 145 (1994);
- G. Bordes and B. van Eijk, Nucl. Phys. **B 435**, 23 (1995);
- T. Stelzer and S. Willenbrock, Phys. Lett. **B 357**, 125 (1995);
- R. Pittau, Phys. Lett. **B 386**, 397 (1996);
- M. C. Smith and S. Willenbrock, Phys. Rev. **D 54**, 6696 (1996);
- D. Atwood, S. Bar-Shalom, G. Eilam and A. Soni, Phys. Rev. **D 54**, 5412 (1996);
- C. S. Li, R. J. Oakes and J. M. Yang, Phys. Rev. **D 55**, 5780 (1997);
- G. Mahlon and S. Parke, Phys. Rev. **D 55**, 7249 (1997);
- A. P. Heinson, A. S. Belyaev and E. E. Boos, Phys. Rev. **D 56**, 3114 (1997);
- T. Stelzer, Z. Sullivan and S. Willenbrock, Phys. Rev. **D 56**, 5919 (1997);
- D. Atwood, S. Bar-Shalom, G. Eilam and A. Soni, Phys. Rev. **D 57**, 2957 (1998);
- T. Stelzer, Z. Sullivan and S. Willenbrock, Phys. Rev. **D 58**, 094021 (1998);
- A.S. Belyaev, E.E. Boos and L.V. Dudko, Phys. Rev. **D 59**, 075001 (1999);
- T. M. P. Tait and C.-P. Yuan, Phys. Rev. **D 63**, 014018 (2000);
- J. A. Aguilar-Saavedra *et al.*, Eur. Phys. J. **C 50**, 519 (2007).
- [14] E. Boos, L. Dudko and T. Ohl, Eur. Phys. J. **C 11**, 473 (1999).
- [15] S. Atağ and B. Şahin, Phys. Rev. **D 73**, 074001 (2006).
- [16] E. Boos, A. Pukhov, M. Sachwitz and H. J. Schreiber, Phys. Lett. **B 404**, 119 (1997);
- J.-J. Cao, *et al.* Phys. Rev. **D 58**, 094004 (1998);
- Q.-H. Cao and J. Wudka, Phys. Rev. **D 74**, 094015 (2006).
- [17] C. Akerlof, Ann Arbor Report No. UM HE 81-59 (1981);
- J. A. Aguilar-Saavedra *et al.*, TESLA Technical Design Report, DESY-2001-011.
- [18] T.L. Barklow, in Proceedings of the 1990 Summer Study on Research Directions for the Decade (Snowmass, Colorado, 1990), and SLAC Report No. SLAC-PUB-5364 (1990).
- [19] I.F. Ginzburg *et al.*, Nucl. Instrum. Methods **205**, 47 (1983); *ibid.* **219**, 5 (1984).
- [20] B. Sahin and I. Sahin, hep-ph/0708.3905.
- [21] T. Kaneko in “New Computing Techniques in Physics Research”, ed. D. Perret-Gallix, W. Wojcik, Edition du CNRS, 1990;
- MINAMI-TATEYA group, “GRACE manual”, KEK Report 92-19, 1993;
- F. Yuasa *et al.*, Prog. Theor. Phys. Suppl. 138 (2000) 18.

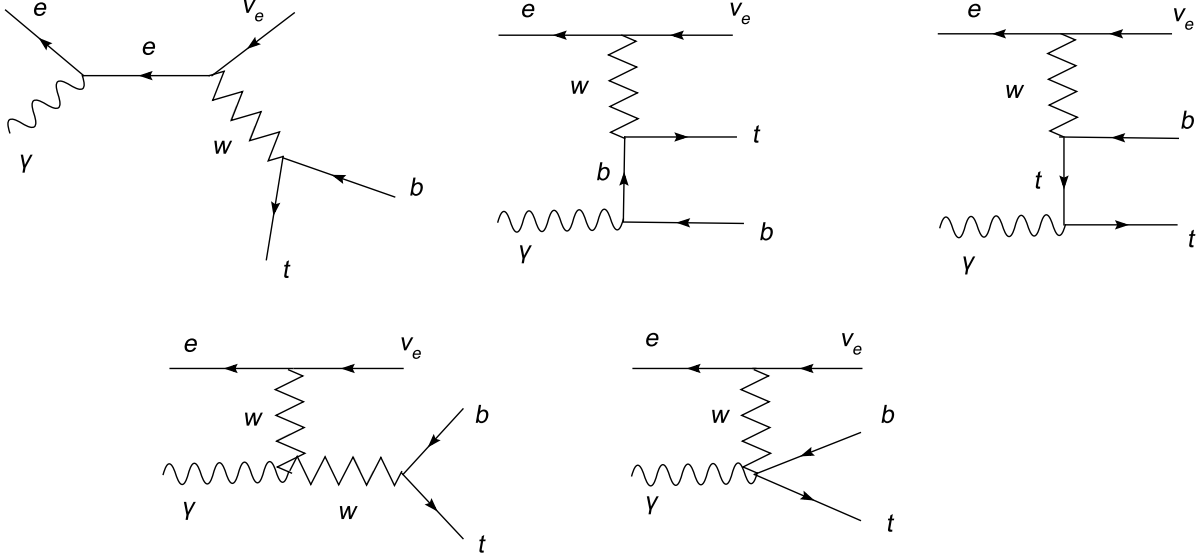


FIG. 1: Tree level Feynmann diagrams for the process  $e^+\gamma \rightarrow t\bar{b}\bar{\nu}_e$ .

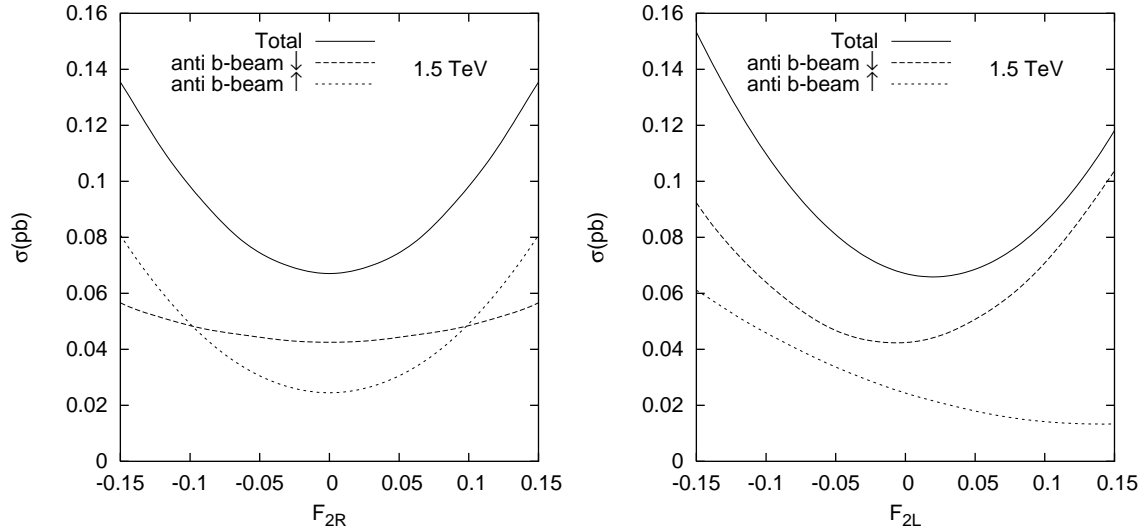


FIG. 2: The integrated cross section of the process  $e^+\gamma \rightarrow t\bar{b}\bar{\nu}_e$  as a function of the anomalous couplings  $F_{2R}$  and  $F_{2L}$  at center of mass energy  $\sqrt{s} = 1.5$  TeV of the parental linear  $e^+e^-$  collider. The top quark spin decomposition axis is along the  $\bar{b}$ -beam.

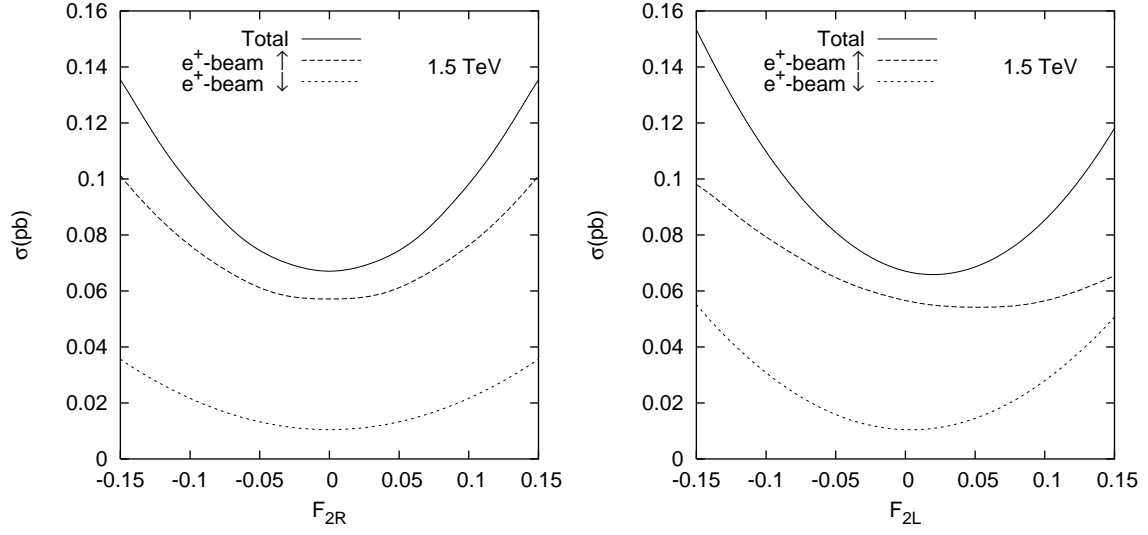


FIG. 3: The same as Fig. 2, but the top quark spin decomposition axis is along the  $e^+$ -beam.

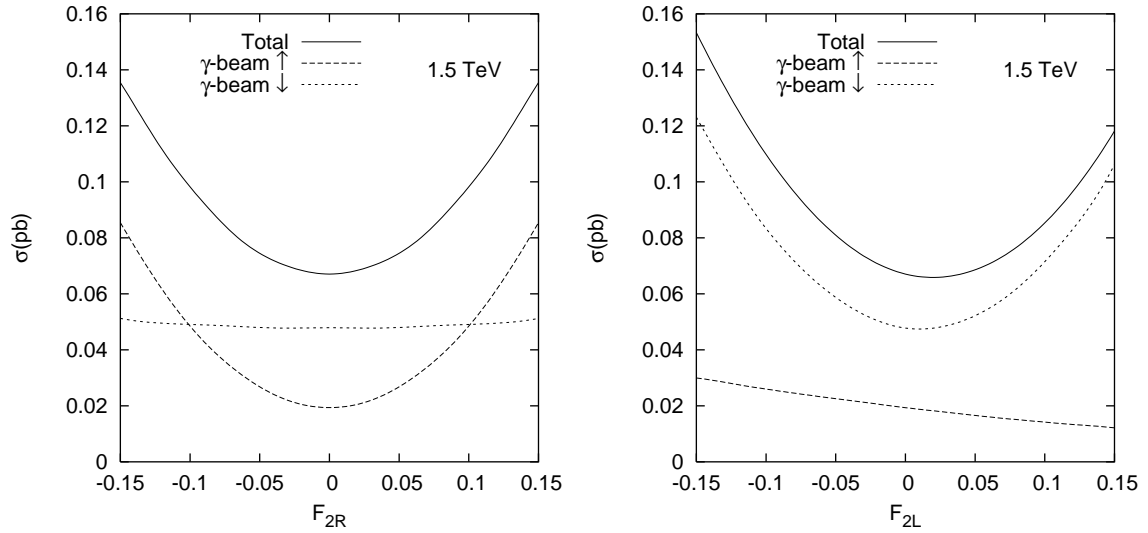


FIG. 4: The same as Fig. 3, but the top quark spin decomposition axis is along the  $\gamma$ -beam.

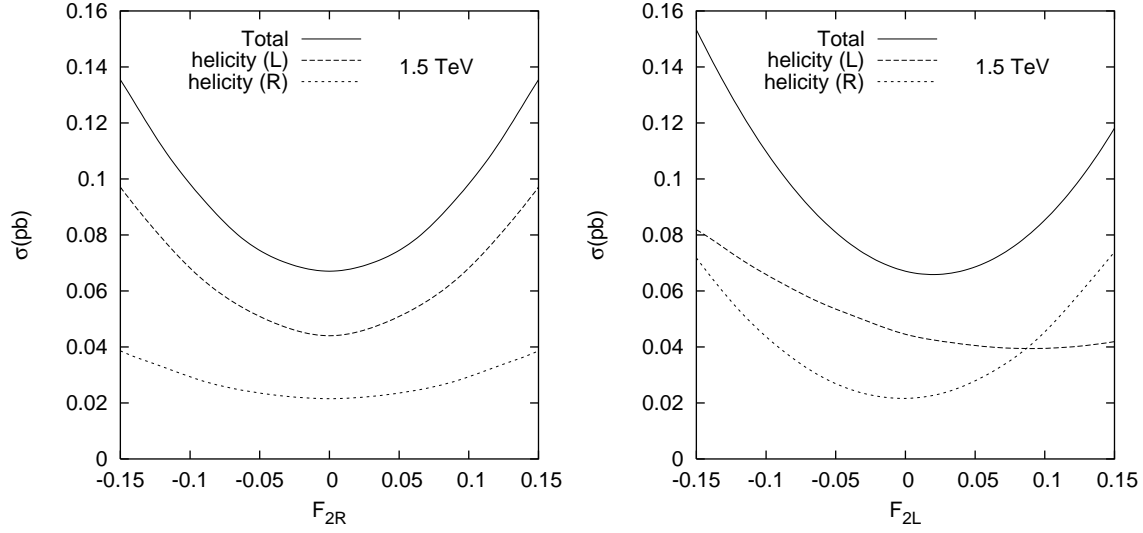


FIG. 5: The same as Fig. 4, but for the top quark helicity basis.

TABLE I: Sensitivity of the  $e\gamma$  collision to anomalous couplings at 95% C.L. for the decomposition axis of the top quark spin along the  $e^+$ -beam,  $\gamma$ -beam,  $\bar{b}$ -beam and helicity directions. Only one of the couplings is assumed to deviate from the SM at a time.  $\sqrt{s} = 0.5$  TeV.

Spin	$F_{2L}$	$F_{2R}$
$e^+$ -beam		
Up	-0.10, 0.08	-0.10, 0.10
Down	-0.06, 0.09	-0.05, 0.05
$\gamma$ -beam		
Up	-0.04, 0.05	-0.05, 0.05
Down	-0.11, 0.05	-0.15, 0.15
$\bar{b}$ -beam		
Up	-0.03, 0.25	-0.07, 0.07
Down	-0.22, 0.04	-0.1, 0.1
Helicity		
Right	-0.16, 0.04	-0.09, 0.09
Left	-0.05, 0.21	-0.08, 0.08
Unpol	-0.08, 0.07	-0.07, 0.07

TABLE II: The same as table I, but for  $\sqrt{s} = 1$  TeV.

Spin	$F_{2L}$	$F_{2R}$
$e^+$ -beam		
Up	-0.02, 0.11	-0.04, 0.04
Down	-0.02, 0.04	-0.03, 0.03
$\gamma$ -beam		
Up	-0.02, 0.02	-0.02, 0.02
Down	-0.02, 0.04	-0.10, 0.10
$\bar{b}$ -beam		
Up	-0.01, 0.30	-0.03, 0.03
Down	-0.05, 0.02	-0.05, 0.05
Helicity		
Right	-0.04, 0.02	-0.04, 0.04
Left	-0.01, 0.21	-0.03, 0.03
Unpol	-0.02, 0.07	-0.03, 0.03

TABLE III: The same as table II, but for  $\sqrt{s} = 1.5$  TeV.

Spin	$F_{2L}$	$F_{2R}$
$e^+$ -beam		
Up	-0.02, 0.12	-0.03, 0.03
Down	-0.01, 0.02	-0.02, 0.02
$\gamma$ -beam		
Up	-0.02, 0.01	-0.02, 0.02
Down	-0.01, 0.03	-0.11, 0.11
$\bar{b}$ -beam		
Up	-0.01, 0.28	-0.02, 0.02
Down	-0.03, 0.02	-0.04, 0.04
Helicity		
Right	-0.02, 0.01	-0.03, 0.03
Left	-0.01, 0.18	-0.02, 0.02
Unpol	-0.01, 0.05	-0.02, 0.02